A_4 lepton flavor model and modulus stabilization from S_4 modular symmetry

Tatsuo Kobayashi,[1] Yusuke Shimizu,[2] Kenta Takagi,[2] Morimitsu Tanimoto,[3] and Takuya H. Tatsuishi[1]

[1]*Department of Physics, Hokkaido University, Sapporo 060-0810, Japan*
[2]*Graduate School of Science, Hiroshima University, Higashi-Hiroshima 739-8526, Japan*
[3]*Department of Physics, Niigata University, Niigata 950-2181, Japan*

(Received 2 October 2019; published 27 December 2019)

We study the modulus stabilization in an A_4 model whose A_4 flavor symmetry is originated from the S_4 modular symmetry. We can stabilize the modulus so that the A_4 invariant superpotential leads to the realistic lepton masses and mixing angles. We also discuss the phenomenological aspect of the present model as a consequence of the modulus stabilization.

DOI: 10.1103/PhysRevD.100.115045

I. INTRODUCTION

The origin of the flavor structure is one of the important mysteries in particle physics. The recent development of the neutrino oscillation experiments provides us with helpful information to investigate the flavor physics. The neutrino oscillation experiments have presented two large flavor mixing angles, which contrast with quark mixing angles. The T2K and NOνA strongly indicate the CP violation in the neutrino oscillation [1,2]. Thus, we are in the era to develop the flavor theory with facing the experimental data.

One of the interesting approaches to understand these phenomena is to impose non-Abelian discrete symmetries for flavors [3–11]. In particular, the A_4 flavor model was examined extensively in the neutrino phenomenology because the A_4 is the minimal group including a triplet irreducible representation, which enables a natural explanation of the existence of three families of leptons [12–18]. However, the origin of A_4 symmetry is unclear.

Geometrical symmetries of compact space in extra dimensional field theories and superstring theory can be origins of non-Abelian discrete flavor symmetries.[1] Torus compactification and orbifold compactification are simple compactifications. These compactifications have the modular symmetry $SL(2,\mathbb{Z})$ as the geometrical symmetry. The shape of the torus is described by the modulus τ, and the modular group transforms the modulus nontrivially. The modular group $SL(2,\mathbb{Z})$ has infinite order, but it includes finite subgroups such as $\Gamma_2 \simeq S_3$, $\Gamma_3 \simeq A_4$, $\Gamma_4 \simeq S_4$, and $\Gamma_5 \simeq A_5$ [24]. Furthermore, the modular group transforms zero modes for each other [25–30]. Thus, the modular symmetry is a sort of flavor symmetry. However, Yukawa couplings, as well as other couplings, are functions of the modulus, and those couplings also transform nontrivially under the modular symmetry.

Inspired by these aspects, recently a new type of flavor model was proposed based on the A_4 modular group [31] in which the modular forms of the weight 2 have been constructed for the A_4 triplet. The successful phenomenological results also have been obtained [32,33]. The modular forms of the weight 2 have been also constructed for S_3 [34], S_4 [35], A_5 [36], $\Delta(96)$, and $\Delta(384)$ [37]. The modular forms of the weight 1 and higher weights are also given for the T' doublet [38]. New types of flavor models towards the flavor origin were studied extensively by use of these modular forms[32,33,39–58].

In minimal model building, we do not need to introduce flavon fields to break flavor symmetries because flavor symmetries are broken when the value of τ is fixed. We can realize lepton and quark masses and mixing angles by choosing a proper value of the modulus τ as well as other parameters of models. It is important how we fix the value of τ, i.e., the modulus stabilization. The modulus value can be fixed as a minimum of scalar potential in the supergravity theory. The modular invariant supergravity theory was studied [59].[2] Indeed, the modulus stabilization was studied by assuming the $SL(2,\mathbb{Z})$ modular invariance for the nonperturbative superpotential in supergravity theory [63,64].[3]

[1]In Refs. [19–23], it was shown that stringy selection rules, in addition to geometrical symmetries, lead to certain non-Abelian flavor symmetries.

[2]See, for their applications, e.g., [60–62].

[3]See also [65].

The purpose of this paper is to study the modulus stabilization and its phenomenological implications in Γ_N flavor models. We consider the modulus stabilization by using the model in Ref. [52] as an illustrating model. Non-Abelian discrete symmetries can be anomalous [66]. (See also, for anomalies of the modular symmetry in concrete models, [67].) For example, S_4 can be anomalous and thus broken down to A_4 by anomalies. In the model of Ref. [52], the S_4 modular symmetry is imposed at the tree level and assumed to be broken to A_4 by anomalies. In this paper, we study an A_4 invariant superpotential of the modulus τ to stabilize it at a supersymmetric minimum of the supergravity scalar potential. We discuss phenomenological aspects in our model.

This paper is organized as follows. In Sec. II, we give a brief review on the modular symmetry and the S_4 anomaly. In Sec. III, we review on the A_4 flavor model in Ref. [52]. In Sec. IV, we study the modulus stabilization in the A_4 model. In Sec. V, we study phenomenological aspects through the modulus stabilization in the A_4 model. Section VI is devoted to our conclusion. Relevant representations of S_4 and A_4 groups are presented in Appendix A. We list the input data of neutrinos in Appendix B. In Appendix C, we show a scenario to induce the modulus potential.

II. MODULAR SYMMETRY AND S_4 ANOMALY

A. Modular symmetry

We give a brief review on the modular symmetry and modular forms. The torus compactification is the simplest compactification. The modulus τ of the torus transforms under the modular transformation as

$$\tau \to \tau' = \gamma\tau = \frac{a\tau + b}{c\tau + d}, \tag{1}$$

where a, b, c, d are integers with satisfying $ad - bc = 1$. This is the symmetry $PSL(2,\mathbb{Z}) = SL(2,\mathbb{Z})/\mathbb{Z}_2$, which is denoted by Γ.

The modular symmetry is generated by two elements, S and T:

$$S\colon\ \tau \to -\frac{1}{\tau}, \qquad T\colon\ \tau \to \tau + 1. \tag{2}$$

They satisfy the following algebraic relations:

$$S^2 = (ST)^3 = \mathbb{I}. \tag{3}$$

Furthermore, we define the congruence subgroups of level N as

$$\Gamma(N) = \left\{ \begin{pmatrix} a & b \\ c & d \end{pmatrix} \in PSL(2,\mathbb{Z}), \right. \\ \left. \begin{pmatrix} a & b \\ c & d \end{pmatrix} = \begin{pmatrix} 1 & 0 \\ 0 & 1 \end{pmatrix} \pmod{N} \right\}. \tag{4}$$

The quotient subgroups Γ_N are given as $\Gamma_N \equiv \Gamma/\Gamma(N)$, and these are finite for $N = 2, 3, 4, 5$, i.e., $\Gamma_2 \simeq S_3$, $\Gamma_3 \simeq A_4$, $\Gamma_4 \simeq S_4$, $\Gamma_5 \simeq A_5$. The algebraic relation $T^N = \mathbb{I}$ is satisfied for $\Gamma(N)$ in addition to Eq. (3).

We study the modular invariant supergravity theory. We use the unit that $M_P = 1$ where M_P denotes the reduced Planck scale. A typical Kähler potential of the modulus field τ is written as follows:

$$K = -\ln[i(\bar{\tau} - \tau)]. \tag{5}$$

The Kähler potential transforms under the modular symmetry as

$$-\ln[i(\bar{\tau} - \tau)] \to -\ln[i(\bar{\tau} - \tau)] + \ln|c\tau + d|^2. \tag{6}$$

Supergravity theory can be written by G,

$$G = K + \ln|W|^2, \tag{7}$$

where W denotes the superpotential in supergravity theory. We require that G is invariant under the modular transformation. The superpotential W therefore transforms as

$$W \to \frac{W}{c\tau + d}, \tag{8}$$

under the modular transformation. That is, the superpotential must be a holomorphic function of the modular weight -1.

Chiral matter fields $\phi^{(I)}$ with the modular weight $-k_I$ transform as

$$(\phi^{(I)})_i(x) \to (c\tau + d)^{-k_I}\rho(\gamma)_{ij}(\phi^{(I)})_j(x), \tag{9}$$

under the modular symmetry, where $\rho(\gamma)_{ij}$ is a unitary matrix in Γ_N. Their Kähler potential can be written as

$$K^{\mathrm{matter}} = \frac{1}{[i(\bar{\tau} - \tau)]^{k_I}}|\phi^{(I)}|^2. \tag{10}$$

Moreover, the modular forms of weight k are the holomorphic functions of τ and transform as

$$f_i(\tau) \to (c\tau + d)^k \rho(\gamma)_{ij} f_j(\tau). \tag{11}$$

The modular forms of $\Gamma(4)$ have been constructed by the use of the Dedekind eta function, $\eta(\tau)$, in Ref. [35].

$$\eta(\tau) = q^{1/24} \prod_{n=1}^{\infty} (1 - q^n), \qquad (12)$$

where $q = e^{2\pi i \tau}$. The modular forms of the weight 2 are written by

$$\begin{aligned} Y_1(\tau) &= Y(1, 1, \omega, \omega^2, \omega, \omega^2 | \tau), \\ Y_2(\tau) &= Y(1, 1, \omega^2, \omega, \omega^2, \omega | \tau), \\ Y_3(\tau) &= Y(1, -1, -1, -1, 1, 1 | \tau), \\ Y_4(\tau) &= Y(1, -1, -\omega^2, -\omega, \omega^2, \omega | \tau), \\ Y_5(\tau) &= Y(1, -1, -\omega, -\omega^2, \omega, \omega^2 | \tau), \end{aligned} \qquad (13)$$

where $\omega = e^{2\pi i/3}$ and

$$\begin{aligned} &Y(a_1, a_2, a_3, a_4, a_5, a_6 \tau) \\ &\quad = a_1 \frac{\eta'(\tau + 1/2)}{\eta(\tau + 1/2)} + 4a_2 \frac{\eta'(4\tau)}{\eta(4\tau)} \\ &\qquad + \frac{1}{4} \sum_{m=0}^{3} a_{m+3} \frac{\eta'((\tau + m)/4)}{\eta((\tau + m)/4)}. \end{aligned} \qquad (14)$$

These five modular forms correspond to reducible representations of $\Gamma_4 \simeq S_4$, and these are decomposed into the **2** and **3**′ representations under S_4,

$$Y_{S_4 \mathbf{2}}(\tau) = \begin{pmatrix} Y_1(\tau) \\ Y_2(\tau) \end{pmatrix}, Y_{S_4 \mathbf{3}'}(\tau) = \begin{pmatrix} Y_3(\tau) \\ Y_4(\tau) \\ Y_5(\tau) \end{pmatrix}. \qquad (15)$$

The generators, S and T, are represented on the above modular forms,

$$\rho(S) = \begin{pmatrix} 0 & \omega \\ \omega^2 & 0 \end{pmatrix}, \qquad \rho(T) = \begin{pmatrix} 0 & 1 \\ 1 & 0 \end{pmatrix}, \qquad (16)$$

for **2**, and

$$\begin{aligned} \rho(S) &= -\frac{1}{3} \begin{pmatrix} -1 & 2\omega^2 & 2\omega \\ 2\omega & 2 & -\omega^2 \\ 2\omega^2 & -\omega & 2 \end{pmatrix}, \\ \rho(T) &= -\frac{1}{3} \begin{pmatrix} -1 & 2\omega & 2\omega^2 \\ 2\omega & 2\omega^2 & -1 \\ 2\omega^2 & -1 & 2\omega \end{pmatrix}, \end{aligned} \qquad (17)$$

for **3**′. The modular forms of higher weights are obtained as the products of $Y_{S_4 \mathbf{2}}(\tau)$ and $Y_{S_4 \mathbf{3}'}(\tau)$. See for other representations in Appendix A.

B. Anomaly

A discrete symmetry can be anomalous like a continuous symmetry [66,68–70]. Each element g in a non-Abelian discrete group satisfies $g^N = 1$, that is, the Abelian Z_N subgroup. If all the Abelian discrete subgroups in a non-Abelian discrete group are anomaly-free, the whole non-Abelian symmetry is anomaly-free [66]. Otherwise, the non-Abelian symmetry is anomalous, and the anomalous subgroup is broken. Furthermore, each element g is represented by a matrix $\rho(g)$. If $\det \rho(g) = 1$, the corresponding Z_N is always anomaly-free. On the other hand, if $\det \rho(g) \neq 1$, the corresponding Z_N symmetry can be anomalous [4,5,66].

In Refs. [4,5], it is shown explicitly which subgroups can be anomalous in non-Abelian discrete symmetries. The S_4 group is isomorphic to $(Z_2 \times Z_2) \rtimes S_3$. The Z_2 symmetry of S_3 can be anomalous in S_4. In general, the **2** and **3** representations as well as **1**′ have $\det \rho(g) = -1$ while the **1** and **3**′ representations have $\det \rho(g) = 1$. Indeed, $\rho(S)$ and $\rho(T)$ for **2** as well as **3** and **1**′ have $\det(\rho(S)) = \det(\rho(T)) = -1$.

If the above Z_2 symmetry in S_4 is anomalous, S_4 is broken to A_4 by anomalies. In this case, S and T themselves are anomalous, but $\tilde{S} = T^2$ and $\tilde{T} = ST$ are anomaly-free. These anomaly-free elements satisfy

$$(\tilde{S})^2 = (\tilde{S}\tilde{T})^3 = (\tilde{T})^3 = \mathbb{I}, \qquad (18)$$

if we impose $T^4 = \mathbb{I}$, that is, the A_4 algebra is realized. The modular forms of weight 2 for S_4 correspond to the A_4 representations as follows:

$$Y_{S_4 \mathbf{2}}(\tau) \to (Y_{A_4 \mathbf{1}'}(\tau), \quad Y_{A_4 \mathbf{1}''}(\tau)), \quad Y_{S_4 \mathbf{3}'}(\tau) \to Y_{A_4 \mathbf{3}}(\tau). \qquad (19)$$

We have

$$\begin{aligned} &Y_{A_4 \mathbf{1}'}(\tau) = Y_1(\tau), \qquad Y_{A_4 \mathbf{1}''}(\tau) = Y_2(\tau), \\ &Y_{A_4 \mathbf{3}}(\tau) = \begin{pmatrix} Y_3(\tau) \\ Y_4(\tau) \\ Y_5(\tau) \end{pmatrix}. \end{aligned} \qquad (20)$$

Note that these are not modular forms of $\Gamma(3)$ because $\tilde{S} = T^2$ and $\tilde{T} = ST$ do not generate $SL(2, \mathbb{Z})$. We can also write S_4 singlet modular forms of weights 4 and 6

$$Y^{(4)}(\tau) = Y_1(\tau) Y_2(\tau), \qquad Y^{(6)}(\tau) = (Y_1(\tau))^3 + (Y_2(\tau))^3. \qquad (21)$$

Both are trivial singlets **1** also under A_4. These are useful for our study.

TABLE I. The charge assignment of $SU(2)$, A_4, and the modular weight ($-k_I$ for fields and k for coupling Y).

	$L_{\mathbf{3}}$	$e^c_{\mathbf{1}}, \mu^c_{\mathbf{1}''}, \tau^c_{\mathbf{1}'}$	H_u	H_d	$Y_{\mathbf{3}}$	$Y_{\mathbf{1}'}$	$Y_{\mathbf{1}''}$
$SU(2)$	2	1	2	2	1	1	1
A_4	3	$1, 1'', 1'$	1	1	3	$1'$	$1''$
$-k_I$	-1	-1	$-1/2$	-1	$k=2$	$k=2$	$k=2$

III. A_4 LEPTON MODEL FROM S_4 MODULAR SYMMETRY

We briefly review on the A_4 lepton flavor model in Ref. [52]. Our A_4 flavor symmetry is originated from the S_4 modular symmetry by assuming that the S_4 symmetry is broken to A_4 by anomalies as mentioned in the previous section.

The model in this paper is described in the supergravity basis where the superpotential has the modular weight -1. On the other hand, the model in Ref. [52] is a global supersymmetric model where the superpotential has the vanishing weight. Thus, we rearrange modular weights of chiral superfields. We assign the modular weight -1 to all of the left-handed and right-handed leptons and Higgs fields.

For the A_4 flavor symmetry, the left-handed lepton doublets, $(L_e, L_\mu, L_\tau)^T$ correspond to the A_4 triplet $L_{\mathbf{3}}$, and the right-handed charged leptons are assigned to the A_4 singlets of $\mathbf{1}, \mathbf{1}'', \mathbf{1}'$, i.e., $e^c_{\mathbf{1}}, \mu^c_{\mathbf{1}''}, \tau^c_{\mathbf{1}'}$, while the up- and down-sector Higgs fields, H_u and H_d, are assigned to the trivial singlet. The charge assignment of the fields and modular forms is summarized in Table I.

The superpotential of the neutrino mass term is given by the Weinberg operator:

$$W_\nu = \frac{1}{\Lambda}[Y_{A_4\mathbf{3}} + aY_{A_4\mathbf{1}'} + bY_{A_4\mathbf{1}''}]L_{\mathbf{3}}L_{\mathbf{3}}H_uH_u, \tag{22}$$

where Λ is a cutoff scale; and parameters a and b are complex constants in general. The superpotential of the mass term of the charged leptons is described as

$$W_e = [\alpha e^c_{\mathbf{1}} + \beta\mu^c_{\mathbf{1}''} + \gamma\tau^c_{\mathbf{1}'}]Y_{A_4\mathbf{3}}L_{\mathbf{3}}H_d, \tag{23}$$

where α, β, and γ are taken to be real and positive without loss of generality.

The superpotential w in the global supersymmetry basis is related to one in the supergravity basis by $|w|^2 = e^K|W|^2$, i.e., $|w_\nu|^2 = |W_\nu|^2/|\tau - \bar{\tau}|$ and $|w_e|^2 = |W_e|^2/|\tau - \bar{\tau}|$.[4] For canonically normalized lepton fields, the Majorana neutrino mass matrix is written as follows:

$$M_\nu = \frac{\langle H_u\rangle^2}{\Lambda'}\left[\begin{pmatrix} 2Y_3 & -Y_5 & -Y_4 \\ -Y_5 & 2Y_4 & -Y_3 \\ -Y_4 & -Y_3 & 2Y_5 \end{pmatrix} + aY_1\begin{pmatrix} 0 & 0 & 1 \\ 0 & 1 & 0 \\ 1 & 0 & 0 \end{pmatrix} + bY_2\begin{pmatrix} 0 & 1 & 0 \\ 1 & 0 & 0 \\ 0 & 0 & 1 \end{pmatrix}\right], \tag{24}$$

where

$$\Lambda' = \Lambda|\tau - \bar{\tau}|^{3/2}, \tag{25}$$

while the charged lepton matrix is given as

$$M_e = \langle H_d\rangle\begin{pmatrix} \alpha' & 0 & 0 \\ 0 & \beta' & 0 \\ 0 & 0 & \gamma' \end{pmatrix}\begin{pmatrix} Y_3 & Y_5 & Y_4 \\ Y_4 & Y_3 & Y_5 \\ Y_5 & Y_4 & Y_3 \end{pmatrix}_{RL}, \tag{26}$$

with

$$\alpha' = \alpha|\tau - \bar{\tau}|^{1/2}, \qquad \beta' = \beta|\tau - \bar{\tau}|^{1/2}, \qquad \gamma' = \gamma|\tau - \bar{\tau}|^{1/2}. \tag{27}$$

The parameters α', β', γ' are determined by the observed charged lepton masses and the value of τ.

We take a and b to be real in order to present a simple viable model. We scan parameters in the following ranges:

$$\tau = [-2.0, 2.0] + i[0.1, 2.8], \qquad a = [-15, 15], \qquad b = [-15, 15], \tag{28}$$

where the fundamental domain of $\Gamma(4)$ is taken into account. The lower-cut 0.1 of $\mathrm{Im}[\tau]$ is artificial to keep the accurate numerical calculation. The upper-cut 2.8 is large enough to estimate the modular forms. We input the experimental data within 3σ C.L. [71] of three mixing angles in the lepton mixing matrix [72] in order to constrain the magnitudes of parameters. We also put the observed neutrino mass ratio $\Delta m^2_{\mathrm{sol}}/\Delta m^2_{\mathrm{atm}}$ and the cosmological bound for the neutrino masses $\sum m_i < 0.12$ [eV] [73,74]. There are two possible spectra of neutrinos masses m_i, which are the normal hierarchy (NH), $m_3 > m_2 > m_1$, and the inverted hierarchy (IH), $m_2 > m_1 > m_3$. Figure 1 shows allowed regions for NH (cyan) and IH (red), respectively.

[4]Here, we treat τ as a vacuum expectation value, but not a holomorphic field.

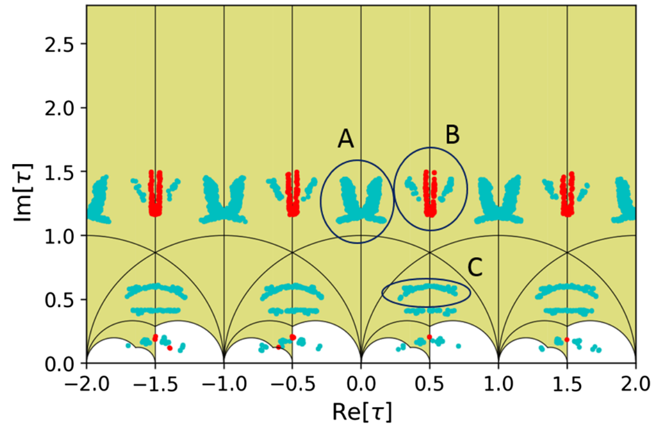

FIG. 1. Allowed regions on the Re[τ]-Im[τ] plane. The fundamental domain of $\Gamma(4)$ is shown by olive green. Cyan points and red points denote the cases of NH and IH, respectively.

IV. MODULUS STABILIZATION

We study the modulus stabilization in the A_4 symmetric model where the S_4 modular symmetry is assumed to be broken by anomalies. For the modulus stabilization, we need a modulus-dependent superpotential $W(\tau)$ which may be induced by nonperturbative effects. Such superpotential $W(\tau)$ must have the modular weight -1 for the modular invariance. However, there is no modular form of odd weights for $\Gamma(4)$. We need some mechanism to generate the superpotential term for modulus stabilization.

Here, we assume that the following superpotential:

$$W = \Lambda_d^{(3)}(Y^{(4)}(\tau))^{-1}, \tag{29}$$

where we assumed that $\Lambda_d^{(3)}$ has the modular weight 3. This modulus superpotential may be induced from the condensation $\langle Q\bar{Q}\rangle \neq 0$ in the hidden sector by strong dynamics such as supersymmetric QCD, and $\Lambda_d^{(3)}$ is the dynamical scale which is related to the condensation, e.g., $\Lambda_d^{(3)} = m\langle Q\bar{Q}\rangle$ (see Appendix C). We assume the above superpotential from the bottom-up viewpoint.

The scalar potential in supergravity theory is written by using K in Eq. (5) and W in Eq. (29) as

$$V = e^K((K_{\tau\bar{\tau}}^{-1}|D_\tau W|^2 - 3|W|^2), \tag{30}$$

where

$$D_\tau W = K_\tau W + W_\tau, \tag{31}$$

with $K_\tau = \partial K/\partial\tau$ and $W_\tau = \partial W/\partial\tau$. We analyze the minimum of the above scalar potential V by examining the stationary condition, $\partial V/\partial\tau = 0$. If there is a solution in the following equation:

$$D_\tau W = 0, \tag{32}$$

we have $\partial V/\partial\tau = 0$. Such a solution is a candidate for the potential minimum and corresponds to a supersymmetric minimum. However, the above scalar potential has no proper supersymmetric minimum. For the slice of $\mathrm{Re}(\tau) = 0$, the value of $|A(\tau)| \equiv |D_\tau W|/\Lambda_d^{(3)}$ is shown in Fig. 2 for larger values of Im[τ]. The value $|D_\tau W|$ vanishes for $\mathrm{Im}[\tau] \to \infty$. Similarly, $|D_\tau W|$ vanishes for $\mathrm{Im}[\tau] \to 0$, because $\mathrm{Im}[\tau] \to 0$ and ∞ are related to each other by the S transformation. The minimum corresponds to $\mathrm{Im}[\tau] \to 0$ and ∞. There is no supersymmetric minimum for a finite value of τ.

On the other hand, the scalar potential has nonsupersymmetric minima as shown in Fig. 3. The minima correspond to $\tau = 1.54i + n$, where n is integer. Unfortunately, these minima do not lead to realistic lepton mass matrices. (See Fig. 1.) We have $V \sim -0.5 \times (\Lambda_d^{(3)})^2$,

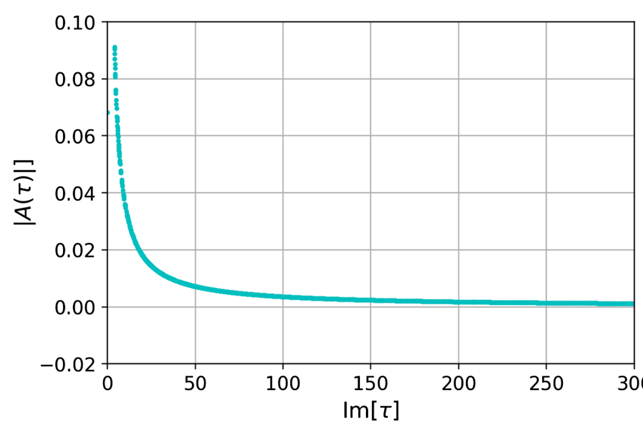

FIG. 2. $|A(\tau)| \equiv |D_\tau W|/\Lambda_d^{(3)}$ at the slice $\mathrm{Re}[\tau] = 0$.

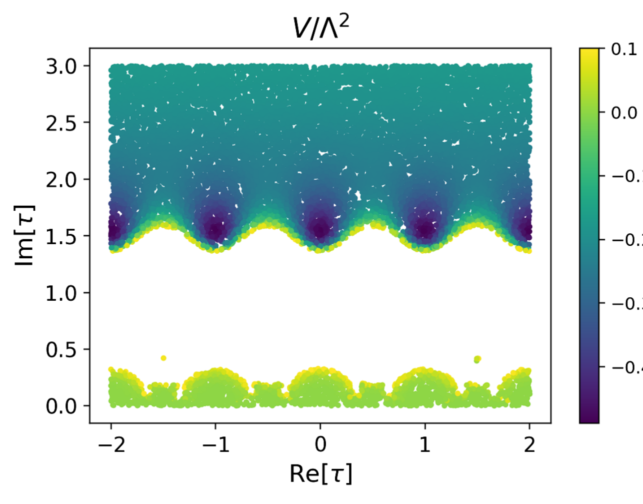

FIG. 3. A contour map of the scalar potential for W in Eq. (29). The potential minima correspond to $\tau = 1.54i + n$, where n is integer.

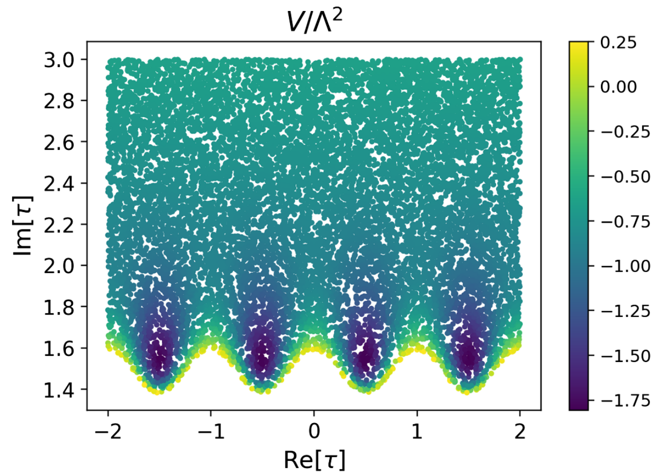

FIG. 4. A contour map of the scalar potential for W in Eq. (33). The potential minima correspond to $\tau = 1.55i + n/2$, where n is odd.

and the modulus mass squared $m_\tau^2 \sim 100 \times (\Lambda_d^{(3)})^2$ at these minima. We need to uplift the vacuum energy by other supersymmetry breaking effects in order to realize almost vanishing vacuum energy $V \approx 0$. Such uplifting effects may not shift significantly the stabilized value $\tau = 1.54i + n$ because the modulus mass squared is large compared with the negative vacuum energy $V \sim -0.5 \times (\Lambda_d^{(3)})^2$.

Alternatively, we assume the following superpotential:

$$W = \Lambda_d^{(-5)} Y^{(4)}(\tau), \tag{33}$$

where we assumed that $\Lambda_d^{(-5)}$ has the modular weight -5. However, the corresponding scalar potential has no proper supersymmetric minimum. Figure 4 shows the corresponding scalar potential. Its minima correspond to $\tau = 1.55i + n/2$, where n is odd. Unfortunately, these values also do not lead to realistic lepton mass matrices. (See Fig. 1.) We have $V \sim -2 \times (\Lambda_d^{(-5)})^2$, and the modulus mass squared $m_\tau^2 \sim 400 \times (\Lambda_d^{(-5)})^2$ at these minima. The effects from uplifting the vacuum energy to $V \approx 0$ on the stabilized value $\tau = 1.55i + n$ is small because the modulus mass squared is large compared with the negative vacuum energy $V \sim -2 \times (\Lambda_d^{(-5)})^2$.

We can use the modular form $Y^{(6)}(\tau)$ instead of $Y^{(4)}(\tau)$ in Eqs. (29) and (33). When we replace $Y^{(4)}(\tau)$ in Eq. (29) by $Y^{(6)}(\tau)$, the corresponding scalar potential has the minimum at $\tau = 1.68i + 1/2$. On the other hand, when we replace $Y^{(4)}(\tau)$ in Eq. (33) by $Y^{(6)}(\tau)$, the corresponding scalar potential has the minimum at $\tau = 1.69i$. Unfortunately, these values of τ are not proper to realize the lepton masses and mixing angles.

Thus, we can stabilize the modulus, but its values are not realistic when the superpotential includes a single modular form. We need more terms to stabilize the modulus at a proper value. For example, we assume the following superpotential:

$$W = \Lambda_d^{(3)}(Y^{(4)}(\tau))^{-1} + \Lambda_d^{(5)}(Y^{(6)}(\tau))^{-1}, \tag{34}$$

where $\Lambda_d^{(5)}$ is assumed to have the modular weight 5. Here, we define $\rho = \Lambda_d^{(5)}/\Lambda_d^{(3)}$. This superpotential always has a supersymmetric minimum for a finite value of ρ. We focus on such a supersymmetric minimum.

For smaller values of τ, the Kähler potential of Eq. (5) may have corrections. Thus, we restrict ourselves to the case with $\tau = \mathcal{O}(1)$. That is, we study the A, B, and C regions in Fig. 1. We can choose a proper value of ρ such that τ is fixed to be a value in the A, B, and C regions through Eq. (32). Figures 5, 6, and 7 show the values of ρ obtained from each value of τ in the A, B, and C regions. The values of τ in the A region are obtained by smaller $|\rho|$.

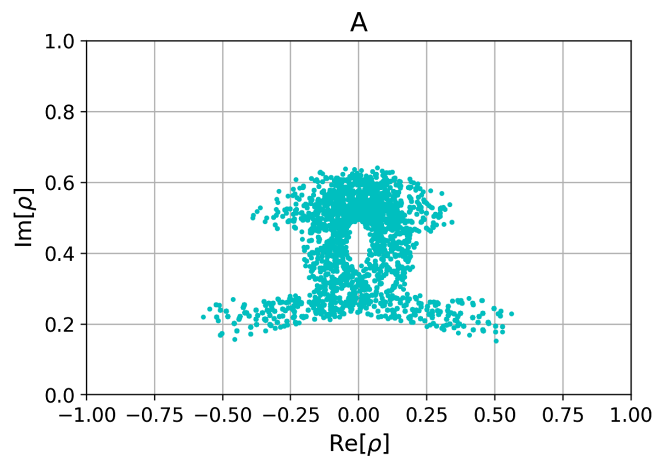

FIG. 5. Values of ρ corresponding to τ in the A region for W in Eq. (34).

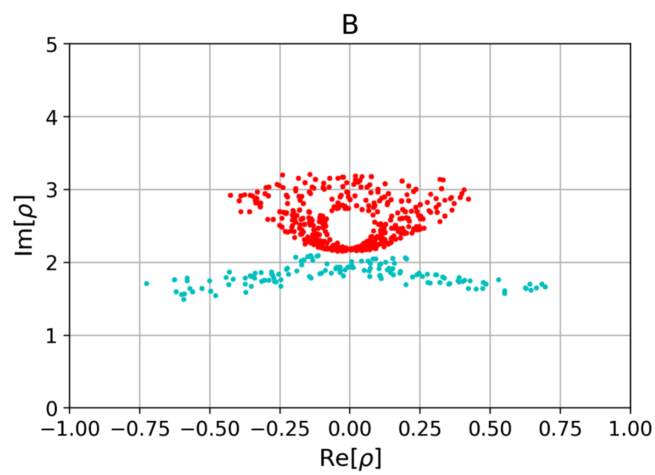

FIG. 6. Values of ρ corresponding to τ in the B region for W in Eq. (34).

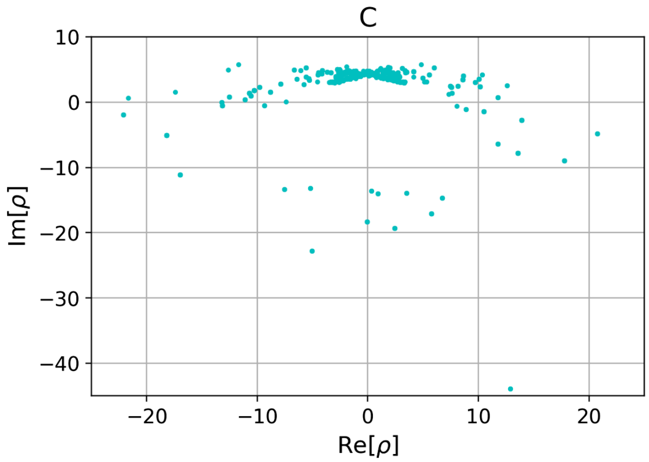

FIG. 7. Values of ρ corresponding to τ in the C region W in Eq. (34).

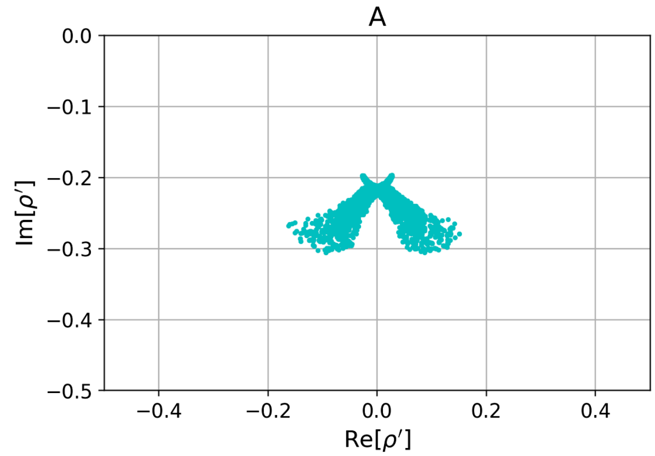

FIG. 8. Values of ρ' corresponding to τ in the A region for W in Eq. (35).

That is, the $Y^{(4)}$ contribution must be larger than the $Y^{(6)}$ contribution. On the other hand, values of τ in the B region are obtained by larger $|\rho|$. Thus, the situation is opposite to the above case. Furthermore, the proper values of ρ for the region C are widely spread. Hence, the A, B, and C regions are realized by quite different values of ρ. At any rate, both $Y^{(4)}(\tau)$ and $Y^{(6)}(\tau)$ are important to fix favorable values of τ in the potential. The IH mass spectrum can be realized only in the B region, that is, $\mathrm{Re}[\rho] \approx [-0.75, 0.75]$ and $\mathrm{Im}[\rho] \approx [2, 3]$.

At these minima, we obtain typical values of $|W_{\tau\tau}| = \mathcal{O}(10) \times \Lambda_d^{(-3)}$ in the A and B regions, while in the C region we can obtain larger $|W_{\tau\tau}| = \mathcal{O}(100) \times \Lambda_d^{(-3)}$. Thus, the modulus mass is estimated $m_\tau = \mathcal{O}(10-100)\Lambda_d^{(-3)}$ in the unit of $M_P = 1$. These minima correspond to the anti–de Sitter supersymmetric vacua whose negative vacuum energy is written by $V = -3e^K|W|^2 = -3|W|^2/|\tau - \bar{\tau}|$. Here, $|W|/\Lambda_d^{(-3)} = \mathcal{O}(1)$ in all of the A, B, and C regions. Thus, the gravitino mass $m_{3/2}$ is estimated by $m_{3/2} = \mathcal{O}(1) \times \Lambda_d^{(-3)}$ in the unit of $M_P = 1$. We need to uplift the vacuum energy to realize almost vanishing vacuum energy, $V \approx 0$ by supersymmetry breaking. Uplifting may shift stabilized values of τ, but such a shift $\delta\tau$ is very small because we can estimate $\delta\tau/\tau \sim m_{3/2}^2/m_\tau^2 = \mathcal{O}(10^{-4} - 10^{-2})$.

Similarly, we can use the following superpotential:

$$W = \Lambda_d^{(-5)} Y^{(4)}(\tau) + \Lambda^{(-7)} Y^{(6)}(\tau), \tag{35}$$

by assuming that nonperturbative effects generate it and $\Lambda_d^{(-5)}$ and $\Lambda_d^{(-7)}$ have the modular weights −5 and −7. Here, we define $\rho' = \Lambda_d^{(-7)}/\Lambda_d^{(-5)}$. Then, similarly we can study the modulus stabilization by using this superpotential. Again, we analyze the supersymmetric condition, Eq. (32). We can find values of the modulus τ, which satisfy the supersymmetric condition, Eq. (32), by choosing a proper value of ρ'. Figures 8, 9, and 10 show such values of ρ' leading to the values of τ in the A, B, and C regions. At these minima, we obtain typical values of $|W_{\tau\tau}| = \mathcal{O}(10)\Lambda_d^{(-5)}$ in the A and B regions, while in the C region we obtain $|W_{\tau\tau}| = \mathcal{O}(10^4)\Lambda_d^{(-5)}$. Therefore, the modulus mass is estimated $m_\tau = \mathcal{O}(10)\Lambda_d^{(-5)}$ in the A and B regions, while the modulus mass can be larger in the C region such as $m_\tau = \mathcal{O}(10^4)\Lambda_d^{(-5)}$. These minima correspond to the anti–de Sitter supersymmetric vacua whose negative vacuum energy is written by $V = -3e^K|W|^2 = -3|W|^2/|\tau - \bar{\tau}|'$, where $|W|/\Lambda_d^{(-5)} = \mathcal{O}(1)$ in the A and B regions and $|W|/\Lambda_d^{(-5)} = \mathcal{O}(10)$ in the C region. The gravitino mass $m_{3/2}$ is estimated by $m_{3/2} = \mathcal{O}(1)\Lambda_d^{(-5)}$ in the A and B regions, and $m_{3/2} = \mathcal{O}(10)\Lambda_d^{(-5)}$ in the C region. Thus, the shift $\delta\tau$ by uplifting will be small.

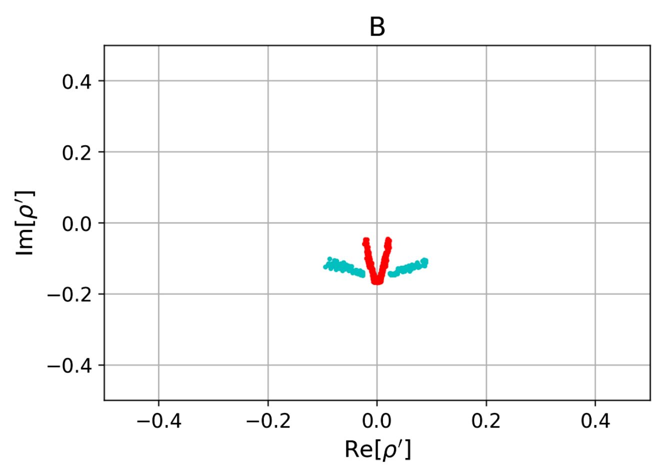

FIG. 9. Values of ρ' corresponding to τ in the B region for W in Eq. (35).

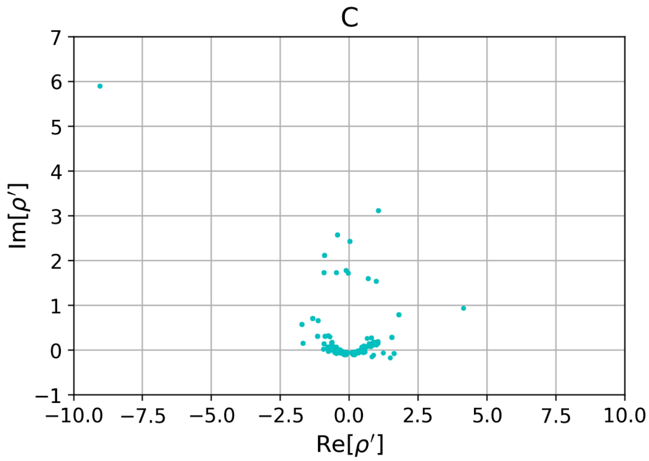

FIG. 10. Values of ρ' corresponding to τ in the C region W in Eq. (35).

As a result, we can stabilize the modulus τ at realistic values in three regions A, B, C by using both the superpotential terms, (34) and (35), with proper values of the parameters, ρ and ρ'. In the next section, we study phenomenological aspects of these three regions following the modulus stabilization by both the superpotential terms, (34) and (35).

V. PHENOMENOLOGICAL ASPECTS OF LEPTONS

In this section, we discuss phenomenological results derived from the mass matrices of charged leptons and neutrinos for three regions A, B, C of the modulus in Fig. 1, respectively.

A. Region of A

Let us present numerical results in the region A of the modulus τ. The parameter ρ to realize the potential minimum for the superpotential (34) is shown in the Re[ρ]-Im[ρ] plane of Fig. 5, while Fig. 8 shows ρ' for the potential minimum for the superpotential (35). In this case, NH is only available.

At first, we show the correlation between δ_{CP} and $\sin^2\theta_{23}$ in Fig. 11. The predicted range of δ_{CP} depends on the value of $\sin^2\theta_{23}$. As $\sin^2\theta_{23}$ increases, the absolute value of δ_{CP} also increases. The range of $|\delta_{CP}| > 95°$ is excluded. Inputting the observed best fit point of $\sin^2\theta_{23} = 0.582$ [71], $|\delta_{CP}|$ is predicted in 50°–90°.

Let us discuss the neutrino mass dependence of δ_{CP}. We present the predicted δ_{CP} versus the sum of neutrino masses $\sum m_i$ in Fig. 12, where the cosmological bound $\sum m_i <$ 120 [meV] is imposed. The predicted δ_{CP} distinctly depends on the sum of neutrino masses, where $\sum m_i >$ 82 [meV]. Near the cosmological bound of $\sum m_i \simeq$ 120 [meV], $|\delta_{CP}|$ is predicted to be 60°–70°.

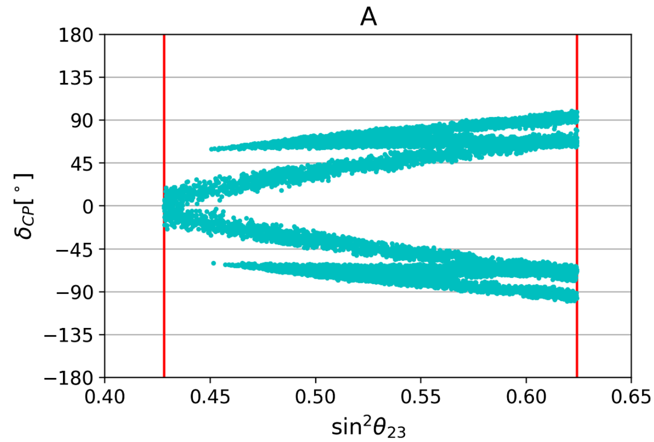

FIG. 11. The predicted region on the $\sin^2\theta_{23}$-δ_{CP} plane in A for NH. Vertical red lines denote 3σ bound of observed data.

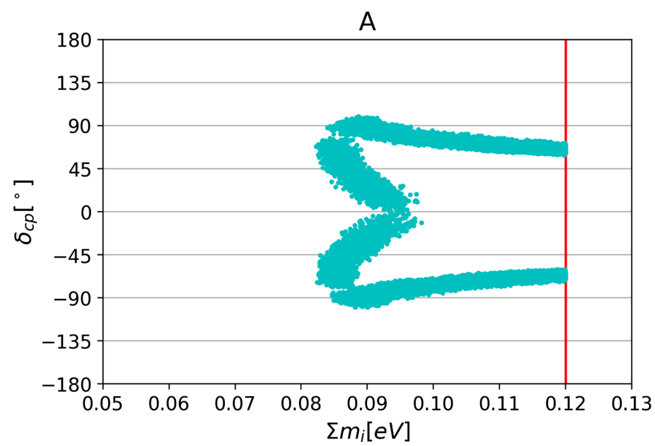

FIG. 12. The sum of neutrino masses $\sum m_i$ dependence of δ_{CP} in A. A vertical red line denotes the cosmological bound.

On the other hand, there is no distinct neutrino mass dependence for $\sin^2\theta_{23}$ as seen in Fig. 13. Near the lower bound of $\sum m_i = 82$ [meV], θ_{23} is predicted in the second octant.

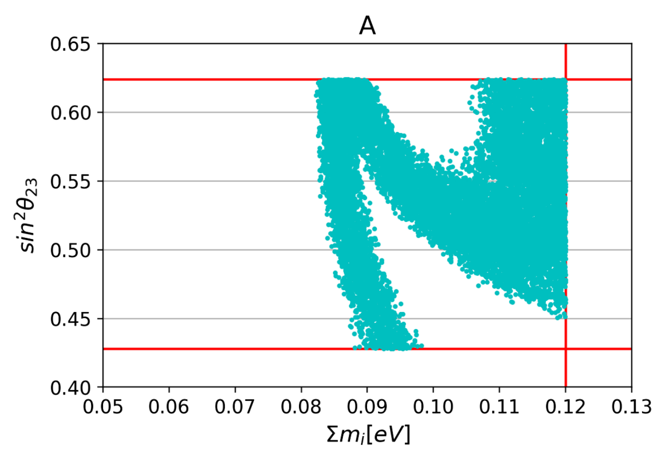

FIG. 13. The sum of neutrino masses $\sum m_i$ dependence of $\sin^2\theta_{23}$ in A.

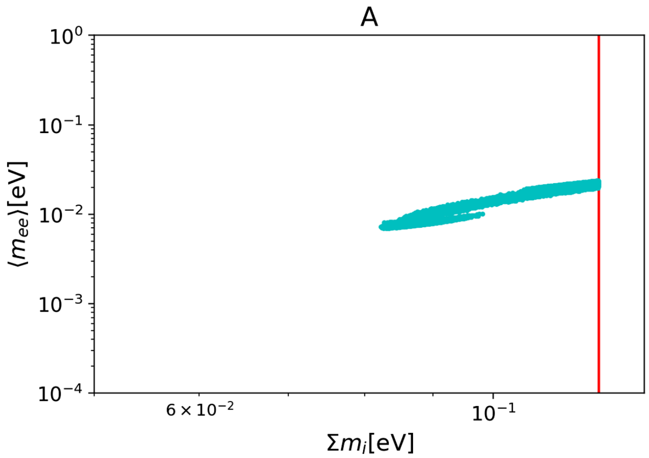

FIG. 14. The predicted effective neutrino mass $\langle m_{ee}\rangle$ versus $\sum m_i$ in A.

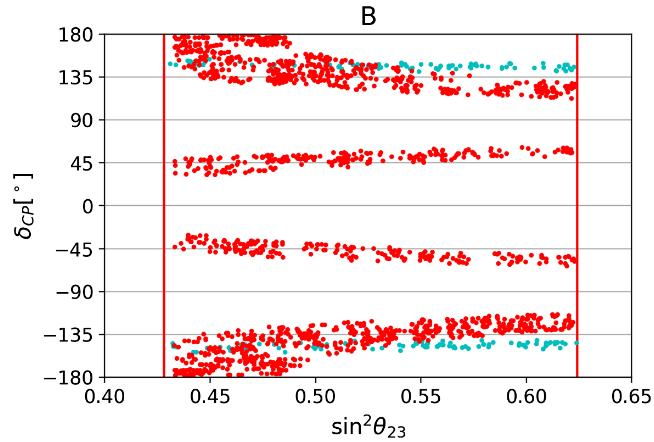

FIG. 15. The predicted region on the $\sin^2\theta_{23}$-δ_{CP} plane in B for NH (cyan) and IH (red). Vertical red lines denote 3σ bound of observed data.

The effective mass of the $0\nu\beta\beta$ decay $\langle m_{ee}\rangle$ is presented in Fig. 14. The prediction is in the range of 6–25 [meV]. We summarize the prediction for $\langle m_{ee}\rangle$ and $\sum m_i$ in Table II.

B. Region of B

We discuss numerical results in the region B of the modulus τ. The parameter ρ to realize the potential minimum for the superpotential (34) is shown in the Re[ρ]-Im[ρ] plane of Fig. 6, while Fig. 9 shows ρ' for the potential minimum for the superpotential (35). In this case, both NH and IH of neutrino masses are available.

We show the correlation between δ_{CP} and $\sin^2\theta_{23}$ in Fig. 15. The distinct prediction of δ_{CP} is given for NH as $\delta_{CP} \simeq \pm 140°$. On the other hand, for IH, δ_{CP} is predicted to be in $\pm[35°–55°]$ and $\pm[110°–180°]$.

We show the predicted δ_{CP} versus the sum of neutrino masses in Fig. 16, which should satisfy the cosmological

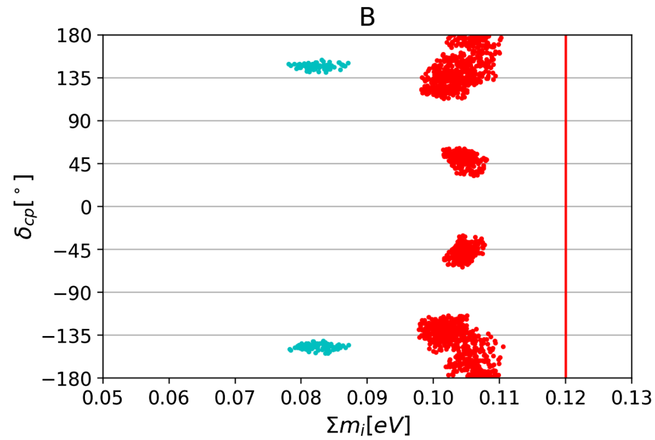

FIG. 16. The sum of neutrino masses $\sum m_i$ dependence of δ_{CP} in B for NH (cyan) and IH (red). A vertical red line denotes the cosmological bound.

bound $\sum m_i < 120$ [meV]. The sum of neutrino masses 78–88 [meV] and 97–110 [meV] for NH and IH, respectively. There is no distinct neutrino mass dependence for $\sin^2\theta_{23}$ as seen in Fig. 17 for both NH and IH cases.

The effective mass of the $0\nu\beta\beta$ decay $\langle m_{ee}\rangle$ is presented in Fig. 18. The prediction is in 9–12 [meV] and 20–35 [meV] for NH and IH, respectively. We summarize the prediction for $\langle m_{ee}\rangle$ and $\sum m_i$ in Table II.

TABLE II. Predicted $\langle m_{ee}\rangle$ and $\sum m_i$ for cases A, B, and C.

	A		B		C	
	NH	IH	NH	IH	NH	IH
$\langle m_{ee}\rangle$ [meV]	6–25	×	9–12	20–35	5–25	×
$\sum m_i$ [meV]	≥ 82	×	78–88	97–110	≥ 88	×

TABLE III. The 3σ ranges of neutrino parameters from NuFIT 4.0 for NH and IH [71].

Observable & 3σ Range for NH	3σ Range for IH	
$\Delta m^2_{\rm atm}$	$(2.431 - 2.622) \times 10^{-3}$ eV^2	$-(2.413–2.606) \times 10^{-3}$ eV^2
$\Delta m^2_{\rm sol}$	$(6.79 - 8.01) \times 10^{-5}$ eV^2	$(6.79 - 8.01) \times 10^{-5}$ eV^2
$\sin^2\theta_{23}$	0.428–0.624	0.433–0.623
$\sin^2\theta_{12}$	0.275–0.350	0.275–0.350
$\sin^2\theta_{13}$	0.02044–0.02437	0.02067–0.02461

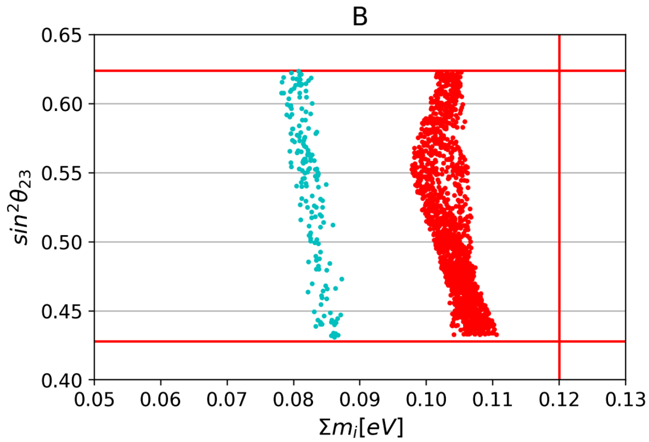

FIG. 17. The sum of neutrino masses $\sum m_i$ dependence of $\sin^2\theta_{23}$ in B for NH (cyan) and IH (red).

C. Region of *C*

Finally, we present numerical discussions in the region C of the modulus τ. The parameter ρ to realize the potential minimum for the superpotential (34) is shown in the Re[ρ]-Im[ρ] plane of Fig. 7, while Fig. 10 shows ρ' for the potential minimum for the superpotential (35). In this case, NH is only available.

We show the correlation between δ_{CP} and $\sin^2\theta_{23}$ in Fig. 19. The predicted δ_{CP} depends on the value of $\sin^2\theta_{23}$. In the second octant of θ_{23}, δ_{CP} is in the range of $\pm[50°, 70°]$.

We show the predicted δ_{CP} versus the sum of neutrino masses in Fig. 20. The predicted δ_{CP} distinctly depends on the sum of neutrino masses, where $\sum m_i > 88$ [meV]. Near the cosmological bound of $\sum m_i \simeq 120$ [meV], $|\delta_{CP}|$ is predicted to be around 70°.

There is also distinct neutrino mass dependence for $\sin^2\theta_{23}$ as seen in Fig. 21. Below $\sum m_i \simeq 102$ [meV], θ_{23} is predicted in the first octant while it is in the second octant in $\sum m_i \geq 110$ [meV].

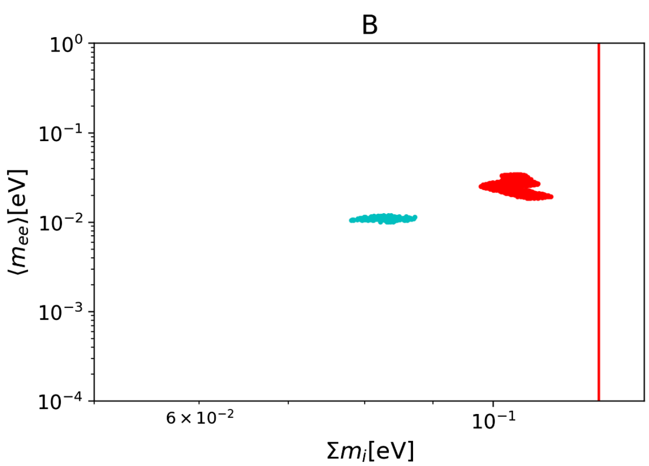

FIG. 18. The predicted effective neutrino mass $\langle m_{ee}\rangle$ versus $\sum m_i$ in B for NH (cyan) and IH (red).

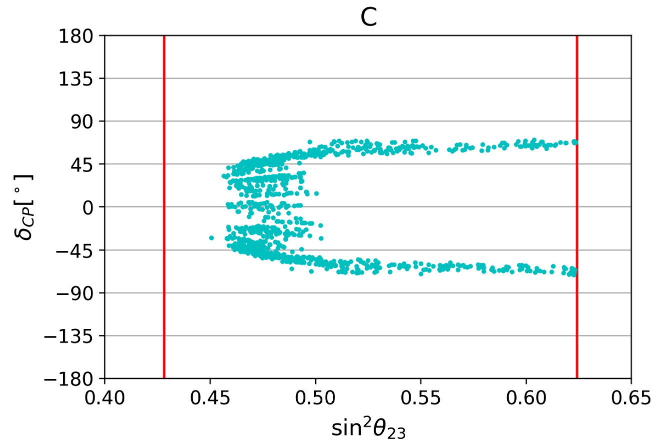

FIG. 19. The predicted region on the $\sin^2\theta_{23}$-δ_{CP} plane in C for NH. Vertical red lines denote 3σ bound of observed data.

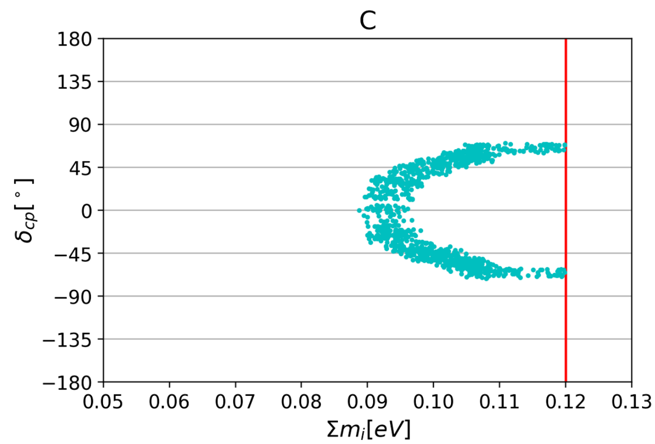

FIG. 20. The sum of neutrino masses $\sum m_i$ dependence of δ_{CP} in C. A vertical red line denotes the cosmological bound.

The effective mass of the $0\nu\beta\beta$ decay $\langle m_{ee}\rangle$ is presented in Fig. 22. The prediction is in the range of 5–25 [meV]. We summarize the prediction for $\langle m_{ee}\rangle$ and $\sum m_i$ in Table II.

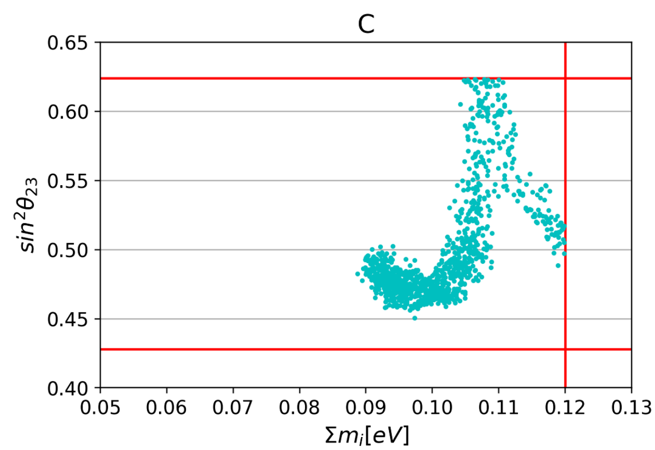

FIG. 21. The sum of neutrino masses $\sum m_i$ dependence of $\sin^2\theta_{23}$ in C.

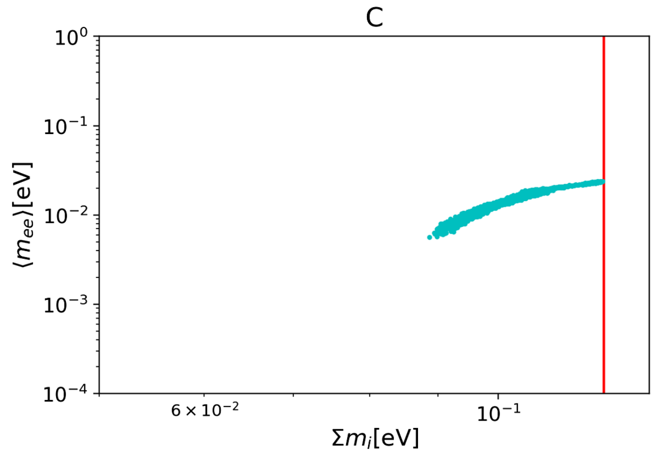

FIG. 22. The predicted effective neutrino mass $\langle m_{ee}\rangle$ versus $\sum m_i$ in C.

VI. CONCLUSION

We have studied the modulus stabilization and its phenomenological aspects in the A_4 flavor model, where the A_4 flavor symmetry is originated from the S_4 modular symmetry. We can stabilize the modulus by a superpotential with a single modular form, but its modulus value is not favorable in lepton masses and mixing angles in the A_4 flavor model. If we assume two modular forms in the superpotential, we can stabilize the modulus at favorable values by using the parameter ρ as well as ρ'. Proper values of ρ and ρ' are of $\mathcal{O}(0.1\text{–}10)$. Thus, contributions due to two modular forms are important in our model. By choosing a proper value of ρ as well as ρ' in the superpotential, we can stabilize the value of τ in our scalar potential such that one can realize the lepton masses and its mixing angles.

We have presented the neutrino phenomenology in the three different regions of τ (A, B, C) where modulus stabilization is realized. The CP violating phase of leptons, δ_{CP} is distinctly predicted in three regions of τ. It is also emphasized that the IH of neutrino masses is reproduced in only the B region. The sum of neutrino masses is predicted in the restricted range for A, B, and C respectively. The cosmological observation of it will provide a crucial test of our model. The effective mass of the $0\nu\beta\beta$ decay $\langle m_{ee}\rangle$ is also predicted. The future experiments can probe our model since our prediction includes $\langle m_{ee}\rangle = 25$ [meV] [75]. Thus, our model realizes the modulus stabilization where the successful phenomenological results are obtained.

ACKNOWLEDGMENTS

This work is supported by MEXT KAKENHI Grant No. JP19H04605 (T. K.), and JSPS Grants-in-Aid for Scientific Research 18J11233 (T. H. T.). The work of Y. S/ is supported by JSPS KAKENHI Grant No. JP17K05418 and Fujyukai Foundation.

APPENDIX A: S_4 AND A_4 REPRESENTATIONS

The representations S and T of $\Gamma_4 \simeq S_4$ are given for the representations **2** and **3′** in Sec. II. Here, we give other representations. The generators S and T are represented by

$$\rho(S) = \frac{1}{3}\begin{pmatrix} -1 & 2\omega^2 & 2\omega \\ 2\omega & 2 & -\omega^2 \\ 2\omega^2 & -\omega & 2 \end{pmatrix},$$
$$\rho(T) = \frac{1}{3}\begin{pmatrix} -1 & 2\omega & 2\omega^2 \\ 2\omega & 2\omega^2 & -1 \\ 2\omega^2 & -1 & 2\omega \end{pmatrix}, \qquad \text{(A1)}$$

on the S_4 **3** representation, where $\omega = e^{i\frac{2}{3}\pi}$, and

$$\rho(S) = \rho(T) = -1, \qquad \text{(A2)}$$

for $\mathbf{1}'$, while $\rho(S) = \rho(T) = 1$ for **1**.

On the other hand, we take the generators of the A_4 group as follows:

$$\rho(S) = \frac{1}{3}\begin{pmatrix} -1 & 2 & 2 \\ 2 & -1 & 2 \\ 2 & 2 & -1 \end{pmatrix},$$
$$\rho(T) = \begin{pmatrix} 1 & 0 & 0 \\ 0 & \omega & 0 \\ 0 & 0 & \omega^2 \end{pmatrix}. \qquad \text{(A3)}$$

In this base, the multiplication rule of the A_4 triplet is

$$\begin{pmatrix} a_1 \\ a_2 \\ a_3 \end{pmatrix}_{\mathbf{3}} \otimes \begin{pmatrix} b_1 \\ b_2 \\ b_3 \end{pmatrix}_{\mathbf{3}} = (a_1b_1 + a_2b_3 + a_3b_2)_{\mathbf{1}} \oplus (a_3b_3 + a_1b_2 + a_2b_1)_{\mathbf{1}'} \oplus (a_2b_2 + a_1b_3 + a_3b_1)_{\mathbf{1}''}$$
$$\oplus \frac{1}{3}\begin{pmatrix} 2a_1b_1 - a_2b_3 - a_3b_2 \\ 2a_3b_3 - a_1b_2 - a_2b_1 \\ 2a_2b_2 - a_1b_3 - a_3b_1 \end{pmatrix}_{\mathbf{3}} \oplus \frac{1}{2}\begin{pmatrix} a_2b_3 - a_3b_2 \\ a_1b_2 - a_2b_1 \\ a_3b_1 - a_1b_3 \end{pmatrix}_{\mathbf{3}},$$
$$\mathbf{1}\otimes\mathbf{1} = \mathbf{1}, \quad \mathbf{1}'\otimes\mathbf{1}' = \mathbf{1}'', \quad \mathbf{1}''\otimes\mathbf{1}'' = \mathbf{1}', \quad \mathbf{1}'\otimes\mathbf{1}'' = \mathbf{1}. \qquad \text{(A4)}$$

More details are shown in the review [4,5].

APPENDIX B: INPUT DATA

We input charged lepton masses in order to constrain the model parameters. We take Yukawa couplings of charged leptons at the grand unified theory scale 2×10^{16} GeV, where $\tan\beta = 2.5$ is taken [32,76–78]:

$$y_e = (1.97 \pm 0.02) \times 10^{-6},$$
$$y_\mu = (4.16 \pm 0.05) \times 10^{-4},$$
$$y_\tau = (7.07 \pm 0.07) \times 10^{-3}, \tag{B1}$$

where lepton masses are given by $m_\ell = \sqrt{2} y_\ell v_H$ with $v_H = 174$ GeV. We also use the following lepton mixing angles and neutrino mass parameters in Table III given by NuFIT 4.0 [71]. The renormalization group equation effects of mixing angles and the mass ratio $\Delta m^2_{\rm sol}/\Delta m^2_{\rm atm}$ are negligibly small in the case of $\tan\beta = 2.5$ for both NH and IH as seen in Appendix E of Ref. [32].

APPENDIX C: MODULUS POTENTIAL

We give a scenario on a plausible mechanism to induce the modulus superpotential. We assume a hidden sector, e.g., supersymmetric QCD which has the $SU(N)$ gauge symmetry and N_f flavors of chiral matter fields, Q_i and $\bar{Q}^j$, with fundamental and antifundamental representations. When $N = N_f$, the mesons $M = Q_i\bar{Q}^j$ and the baryon $B = \epsilon^{i_1\cdots i_N} Q_{i_1}\cdots Q_{i_N}$ as well as the antibaryon condensate [79]. If the superpotential at the tree level has the mass term, $W = m^i_j Q_i \bar{Q}^j$, the above condensation leads to the term $W = m\langle M\rangle$. Suppose that the M has the modular weight $-k-1$. The mass parameter must be a modular form of the weight k since the modular invariance requires that m has the modular weight k. The following superpotential may be induced

$$W = cY^{(k)}(\tau)\langle M\rangle. \tag{C1}$$

If there is another hidden sector to condensate, we may realize the superpotential

$$W = cY^{(k)}(\tau)\langle M\rangle + c'Y^{(k')}(\tau)\langle M'\rangle, \tag{C2}$$

where we assume that another meson fields M' has the modular weight $-k'-1$. Furthermore, the condensation of the baryon B may induce another term with a different modular weight.

[1] K. Abe *et al.* (T2K Collaboration), Phys. Rev. Lett. **121**, 171802 (2018).
[2] M. A. Acero *et al.* (NOvA Collaboration), Phys. Rev. D **98**, 032012 (2018).
[3] G. Altarelli and F. Feruglio, Rev. Mod. Phys. **82**, 2701 (2010).
[4] H. Ishimori, T. Kobayashi, H. Ohki, Y. Shimizu, H. Okada, and M. Tanimoto, Prog. Theor. Phys. Suppl. **183**, 1 (2010).
[5] H. Ishimori, T. Kobayashi, H. Ohki, H. Okada, Y. Shimizu, and M. Tanimoto, Lect. Notes Phys. **858**, 87 (2012).
[6] D. Hernandez and A. Y. Smirnov, Phys. Rev. D **86**, 053014 (2012).
[7] S. F. King and C. Luhn, Rep. Prog. Phys. **76**, 056201 (2013).
[8] S. F. King, A. Merle, S. Morisi, Y. Shimizu, and M. Tanimoto, New J. Phys. **16**, 045018 (2014).
[9] M. Tanimoto, AIP Conf. Proc. **1666**, 120002 (2015).
[10] S. F. King, Prog. Part. Nucl. Phys. **94**, 217 (2017).
[11] S. T. Petcov, Eur. Phys. J. C **78**, 709 (2018).
[12] E. Ma and G. Rajasekaran, Phys. Rev. D **64**, 113012 (2001).
[13] K. S. Babu, E. Ma, and J. W. F. Valle, Phys. Lett. B **552**, 207 (2003).
[14] G. Altarelli and F. Feruglio, Nucl. Phys. **B720**, 64 (2005).
[15] G. Altarelli and F. Feruglio, Nucl. Phys. **B741**, 215 (2006).
[16] Y. Shimizu, M. Tanimoto, and A. Watanabe, Prog. Theor. Phys. **126**, 81 (2011).
[17] S. T. Petcov and A. V. Titov, Phys. Rev. D **97**, 115045 (2018).
[18] S. K. Kang, Y. Shimizu, K. Takagi, S. Takahashi, and M. Tanimoto, Prog. Theor. Exp. Phys. **2018**, 083B01 (2018).
[19] T. Kobayashi, H. P. Nilles, F. Ploger, S. Raby, and M. Ratz, Nucl. Phys. **B768**, 135 (2007).
[20] T. Kobayashi, S. Raby, and R. J. Zhang, Nucl. Phys. **B704**, 3 (2005).
[21] P. Ko, T. Kobayashi, J. h. Park, and S. Raby, Phys. Rev. D **76**, 035005 (2007); **76**, 059901(E) (2007).
[22] F. Beye, T. Kobayashi, and S. Kuwakino, Phys. Lett. B **736**, 433 (2014).
[23] H. Abe, K. S. Choi, T. Kobayashi, and H. Ohki, Nucl. Phys. **B820**, 317 (2009).
[24] R. de Adelhart Toorop, F. Feruglio, and C. Hagedorn, Nucl. Phys. **B858**, 437 (2012).
[25] J. Lauer, J. Mas, and H. P. Nilles, Phys. Lett. B **226**, 251 (1989); Nucl. Phys. **B351**, 353 (1991).
[26] W. Lerche, D. Lust, and N. P. Warner, Phys. Lett. B **231**, 417 (1989).
[27] S. Ferrara, D. Lust, and S. Theisen, Phys. Lett. B **233**, 147 (1989).
[28] T. Kobayashi and S. Nagamoto, Phys. Rev. D **96**, 096011 (2017).
[29] T. Kobayashi, S. Nagamoto, S. Takada, S. Tamba, and T. H. Tatsuishi, Phys. Rev. D **97**, 116002 (2018).

[30] A. Baur, H. P. Nilles, A. Trautner, and P. K. S. Vaudrevange, Phys. Lett. B **795**, 7 (2019); Nucl. Phys. **B947**, 114737 (2019).
[31] F. Feruglio, arXiv:1706.08749.
[32] J. C. Criado and F. Feruglio, SciPost Phys. **5**, 042 (2018).
[33] T. Kobayashi, N. Omoto, Y. Shimizu, K. Takagi, M. Tanimoto, and T. H. Tatsuishi, J. High Energy Phys. 11 (2018) 196.
[34] T. Kobayashi, K. Tanaka, and T. H. Tatsuishi, Phys. Rev. D **98**, 016004 (2018).
[35] J. T. Penedo and S. T. Petcov, Nucl. Phys. **B939**, 292 (2019).
[36] P. P. Novichkov, J. T. Penedo, S. T. Petcov, and A. V. Titov, J. High Energy Phys. 04 (2019) 174.
[37] T. Kobayashi and S. Tamba, Phys. Rev. D **99**, 046001 (2019).
[38] X. G. Liu and G. J. Ding, J. High Energy Phys. 08 (2019) 134.
[39] P. P. Novichkov, J. T. Penedo, S. T. Petcov, and A. V. Titov, J. High Energy Phys. 04 (2019) 005.
[40] F. J. de Anda, S. F. King, and E. Perdomo, arXiv:1812.05620.
[41] H. Okada and M. Tanimoto, Phys. Lett. B **791**, 54 (2019).
[42] T. Kobayashi, Y. Shimizu, K. Takagi, M. Tanimoto, T. H. Tatsuishi, and H. Uchida, Phys. Lett. B **794**, 114 (2019).
[43] P. P. Novichkov, S. T. Petcov, and M. Tanimoto, Phys. Lett. B **793**, 247 (2019).
[44] G. J. Ding, S. F. King, and X. G. Liu, arXiv:1903.12588.
[45] T. Nomura and H. Okada, Phys. Lett. B **797**, 134799 (2019).
[46] P. P. Novichkov, J. T. Penedo, S. T. Petcov, and A. V. Titov, J. High Energy Phys. 07 (2019) 165.
[47] H. Okada and M. Tanimoto, arXiv:1905.13421.
[48] I. de Medeiros Varzielas, S. F. King, and Y. L. Zhou, arXiv:1906.02208.
[49] T. Nomura and H. Okada, arXiv:1906.03927.
[50] T. Kobayashi, Y. Shimizu, K. Takagi, M. Tanimoto, and T. H. Tatsuishi, arXiv:1906.10341.
[51] H. Okada and Y. Orikasa, arXiv:1907.04716.
[52] T. Kobayashi, Y. Shimizu, K. Takagi, M. Tanimoto, and T. H. Tatsuishi, arXiv:1907.09141.
[53] G. J. Ding, S. F. King, and X. G. Liu, J. High Energy Phys. 09 (2019) 074.
[54] H. Okada and Y. Orikasa, arXiv:1907.13520.
[55] S. F. King and Y. L. Zhou, arXiv:1908.02770.
[56] T. Nomura, H. Okada, and O. Popov, arXiv:1908.07457.
[57] H. Okada and Y. Orikasa, arXiv:1908.08409.
[58] J. C. Criado, F. Feruglio, and S. J. D. King, arXiv:1908.11867.
[59] S. Ferrara, D. Lust, A. D. Shapere, and S. Theisen, Phys. Lett. B **225**, 363 (1989).
[60] J. P. Derendinger, S. Ferrara, C. Kounnas, and F. Zwirner, Nucl. Phys. **B372**, 145 (1992).
[61] L. E. Ibanez and D. Lust, Nucl. Phys. **B382**, 305 (1992).
[62] T. Kobayashi, S. Nagamoto, and S. Uemura, Prog. Theor. Exp. Phys. **2017**, 023B02 (2017).
[63] S. Ferrara, N. Magnoli, T. R. Taylor, and G. Veneziano, Phys. Lett. B **245**, 409 (1990).
[64] M. Cvetic, A. Font, L. E. Ibanez, D. Lust, and F. Quevedo, Nucl. Phys. **B361**, 194 (1991).
[65] T. Kobayashi, D. Nitta, and Y. Urakawa, J. Cosmol. Astropart. Phys. 08 (2016) 014.
[66] T. Araki, T. Kobayashi, J. Kubo, S. Ramos-Sanchez, M. Ratz, and P. K. S. Vaudrevange, Nucl. Phys. **B805**, 124 (2008).
[67] Y. Kariyazono, T. Kobayashi, S. Takada, S. Tamba, and H. Uchida, Phys. Rev. D **100**, 045014 (2019).
[68] L. M. Krauss and F. Wilczek, Phys. Rev. Lett. **62**, 1221 (1989).
[69] L. E. Ibanez and G. G. Ross, Phys. Lett. B **260**, 291 (1991).
[70] T. Banks and M. Dine, Phys. Rev. D **45**, 1424 (1992).
[71] NuFIT 4.0, www.nu-fit.org (2018); I. Esteban, M. C. Gonzalez-Garcia, M. Maltoni, I. Martinez-Soler, and T. Schwetz, J. High Energy Phys. 01 (2017) 087.
[72] M. Tanabashi *et al.* (Particle Data Group), Phys. Rev. D **98**, 030001 (2018).
[73] S. Vagnozzi, E. Giusarma, O. Mena, K. Freese, M. Gerbino, S. Ho, and M. Lattanzi, Phys. Rev. D **96**, 123503 (2017).
[74] N. Aghanim *et al.* (Planck Collaboration), arXiv:1807.06209.
[75] Y. Gando (KamLAND-Zen Collaboration), arXiv:1904.06655.
[76] S. Antusch, J. Kersten, M. Lindner, M. Ratz, and M. A. Schmidt, J. High Energy Phys. 03 (2005) 024.
[77] S. Antusch and V. Maurer, J. High Energy Phys. 11 (2013) 115.
[78] F. Björkeroth, F. J. de Anda, I. de Medeiros Varzielas, and S. F. King, J. High Energy Phys. 06 (2015) 141.
[79] K. A. Intriligator and N. Seiberg, Nucl. Phys. B, Proc. Suppl. **45**, 1 (1996); Subnuclear series **34**, 237 (1997).